Cite as: Korzeń M, Nowakowska-Płaza A, Leszkiewicz M, Sudoł-Szopińska I: Imaging methods in monitoring gout – a pictorial essay. J Ultrason 2024; 24: 22. doi: 10.15557/JoU.2024.0022.

Submitted: 01.10.2023
Accepted: 11.04.2024
Published: 28.06.2024

Imaging methods in monitoring gout – a pictorial essay

Maria Korzeń[1], Anna Nowakowska-Płaza[2], Marek Leszkiewicz[1], Iwona Sudoł-Szopińska[1]

[1] *Department of Radiology, National Institute of Geriatrics, Rheumatology and Rehabilitation, Poland*
[2] *Department of Rheumatology, National Institute of Geriatrics, Rheumatology and Rehabilitation, Poland*

Corresponding author: Maria Korzeń; e-mail: m.sotniczuk@gmail.com

DOI: 10.15557/JoU.2024.0022

Keywords
DECT; ultrasound; gout; dual-energy computed tomography

Abstract

We present a pictorial essay based on the case of a 52-year-old man suffering from chronic gout, who was followed up for seven years. During this period of time, radiographs, ultrasonography, and dual-energy computed tomography were performed several times, revealing severe progression of gout. This was most likely due to the lack of patient compliance. Inflammatory and destructive lesions were observed in the wrists, in the metacarpophalangeal and proximal interphalangeal joints. Ultrasonography showed tenosynovitis, synovitis with small calcifications in the synovial membrane. Radiographs obtained in later stages showed tophi and bone erosions. Dual-energy computed tomography showed deposits of monosodium urate crystals in different locations, which increased in volume over time. This modality can be used to confirm a clinical diagnosis of gout, especially in early stages of the disease, and to follow up the treatment.

Introduction

Gout is the most widespread crystal arthropathy with increasing prevalence in developed societies, and a common cause of joint pain. It is caused by deposition of monosodium urate (MSU) crystals mainly in joints and periarticular soft tissues. Gout usually presents with an acute onset of joint pain and swelling, with a predilection to the 1st metatarsal joint (MTP)[1]. It can proceed to the chronic subtype causing joint destruction. A 'typical' gout patient is a man in his 50s, with an excessive purine intake in his diet and with metabolic syndrome[2–4]. Diagnosis of gout is established on the basis of clinical, laboratory and imaging findings. The gold standard for the diagnosis is detection of negatively birefringent MSU crystals under polarizing microscopy in synovial fluid[5]. Joint aspiration is an invasive procedure and can provide false negative results, especially in an early stage of the disease[2]. Modalities with the highest sensitivity and specificity include the ultrasound (US) and dual-energy computed tomography (DECT)[6,7]. Features of early gout in ultrasound include effusion in the affected joints with the snowstorm sign, synovial hypertrophy, bursitis, and a "double contour sign"[2,7]. DECT enables the detection of very small deposits of MSU crystals. It shows their exact location and calculates their volume[8]. In chronic gout, both previously mentioned methods, as well as radiography, are useful in clinical practice. Features of chronic gout on radiographs include tophi, erosions, and pathological microfractures[9,10]. US can also reveal tophi, erosions, and tendinopathy[2,7]. In this pictorial essay, we present a patient who had multiple imaging studies performed over a period of time, including DECT, US, and radiographs. This allowed us to see the progression of the disease and track changes in crystal deposition in individual joints.

Pictorial essay

A 52-year-old patient was admitted to rheumatologic department due to worsening of gout symptoms (multiple joint pain and swelling). The patient suffered from gout for over 30 years and was treated with multiple medications including allopurinol, febuxostat, colchicine, non-steroidal anti-inflammatory drugs (NSAIDs), and steroids. His comorbidities included metabolic syndrome (obesity with BMI >35, hypertension, hypertriglyceridemia, and low HDL level), type 2 diabetes, renal calcinosis, and sleep apnea. He was hospitalized several times due to gout flares in our site and had multiple imaging studies performed. This allowed us to monitor the progression of gout and assess his response to treatment.

In 2015, radiographs of the patient's feet showed advanced degenerative changes, with multiple geodes in the 1st MTP joints, geodes and erosions in the head of the 5th metatarsal bilaterally (Fig. 1).

Hand radiographs showed bilateral changes including geodes in the styloid process of the ulna, narrowing of intra-articular spaces in the

© 2024 Authors. This is an open-access article distributed under the terms of the Creative Commons Attribution-NonCommercial-NoDerivatives License (CC BY-NC-ND). Reproduction is permitted for personal, educational, non-commercial use, provided that the original article is in whole, unmodified, and properly cited.

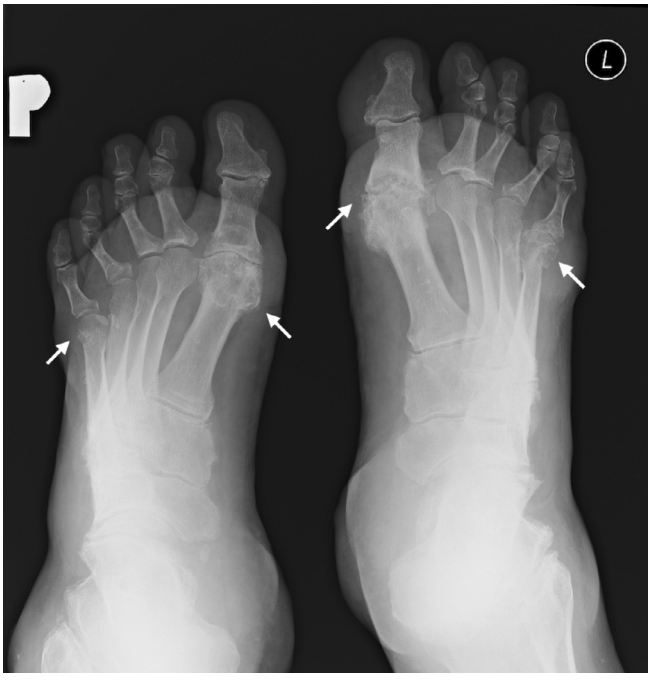

Fig. 1. *Radiography of feet, AP projection, year 2015. Advanced degenerative changes, with multiple geodes in the 1st MTP joints, geodes and erosions in head of 5th metatarsal bilaterally, arrows*

radiocarpal joints, and degenerative changes in the interphalangeal joints, as well as a small contracture in the 2nd proximal interphalangeal (PIP) joint of the right hand (Fig. 2).

The patient was advised to take allopurinol and colchicine on a daily basis. Prednisone was added for gout attacks. Unfortunately, the patient modified the doses without consulting his doctor and did not follow a low-purine diet.

Four years later, radiographs showed progression of the illness. In addition to the previously observed lesions, there was a thickening of soft tissues in the fingers in both hands and significant contractures in the 2nd PIP joints now of both hands (Fig. 3).

Ultrasound of the right hand showed thickening of the synovial membrane in the radiocarpal joint with tiny echogenic foci embedded in the synovium, presumably representing crystals, with no hyperemia (Fig. 4).

Chronic tenosynovitis was present in the 2nd, 3rd, 4th, and 6th extensor compartments of the wrist (Fig. 5).

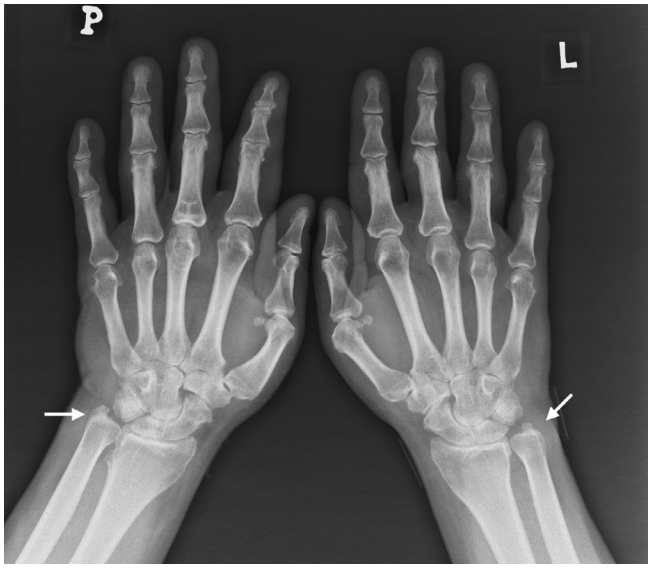

Fig. 2. *Radiography of hands in pronation, PA projection, year 2015. Geodes in styloid process of ulna bilaterally, narrowing of intra-articular spaces in the radiocarpal joint bilaterally, degenerative changes in the interphalangeal joints and a small contracture in the 2nd proximal interphalangeal (PIP) joint of the right hand, arrows*

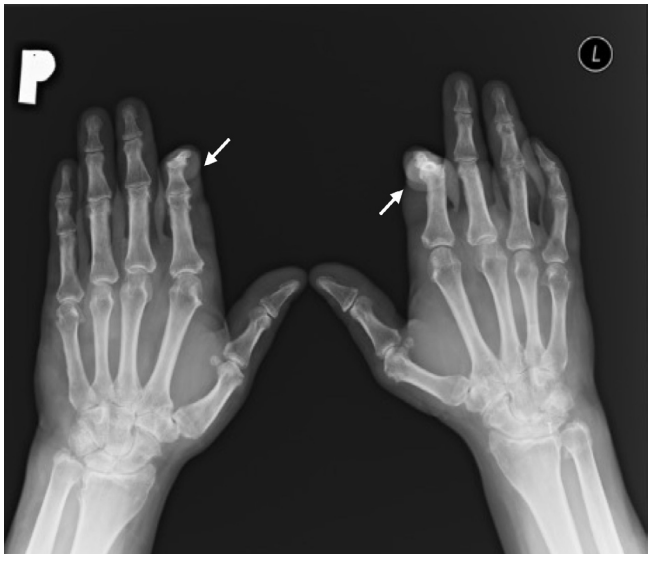

Fig. 3. *Radiography of hands in pronation, PA projection, year 2019. Thickening of soft tissues and contractures in 2nd PIP joints bilaterally, arrows*

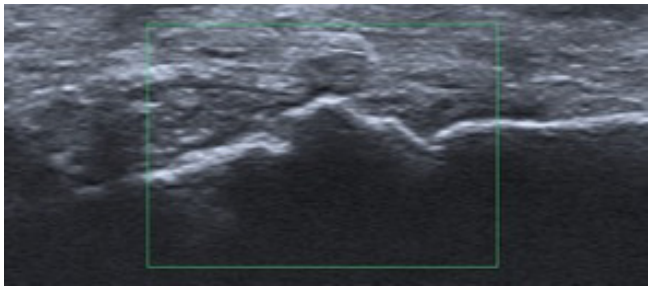

Fig. 4. *Ultrasound of the right hand shows thickening of the synovial membrane in the radiocarpal joint, with crystals and without hyperemia*

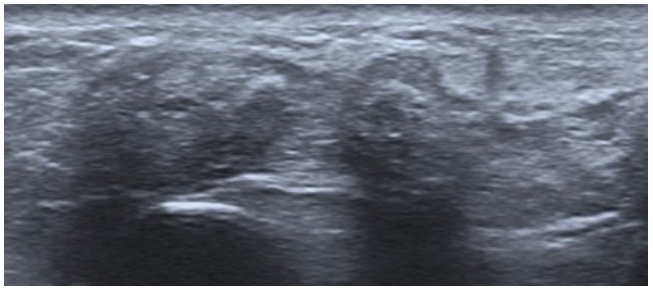

Fig. 5. *Ultrasound of the right hand shows hyperechoic content with tiny calcifications in the tenosynovium of the 3rd and 4th extensor compartments*

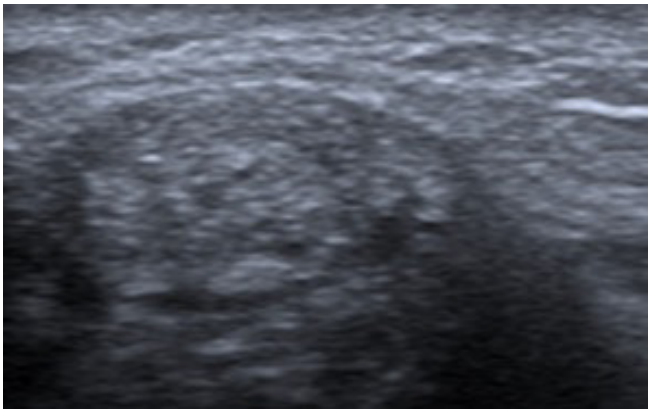

Fig. 6. *Tophus of high echogenicity, with tiny echogenic foci representing crystals (a "starry sky" sign) in the 6th compartment of the extensors*

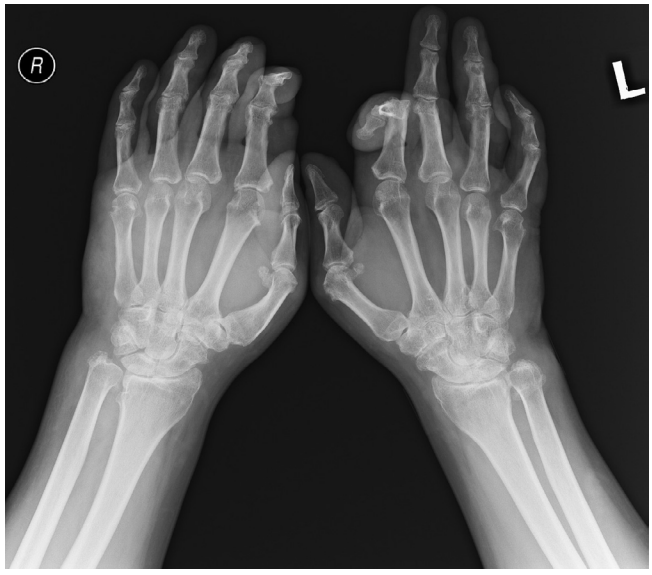

Fig. 8. *Radiography of the hands in pronation, PA projection, year 2021. Progression of contractures in the 2nd fingers*

A hyperechoic nodule representing a tophus with tiny crystals (a "starry sky" sign) was seen on the level of distal radioulnar joint (Fig. 6).

Since the progression of the patient's illness was significant, DECT of the patient's hands was performed. It showed MSU crystals deposits in both hands. The total amount of deposits was calculated to be 1.67 cm^3 in the left hand and 5.29 cm^3 in the right hand. Deposits were noted mainly around the metacarpophalangeal (MCP) joints and in the wrists (Fig. 7).

Accordingly, lesinurad 200 mg/24 h was added to the patient's treatment regime.

In 2021, the patient was readmitted due to worsening of symptoms. Radiography of the hands was similar to the previous examination, from 2019, except for the progression of contractures in the 2nd fingers (Fig. 8).

DECT of hands was performed again. It revealed a significant increase in the amount of MSU crystals by 5.64 cm^3 in the left hand and by 11.99 cm^3 in the right hand (Fig. 9).

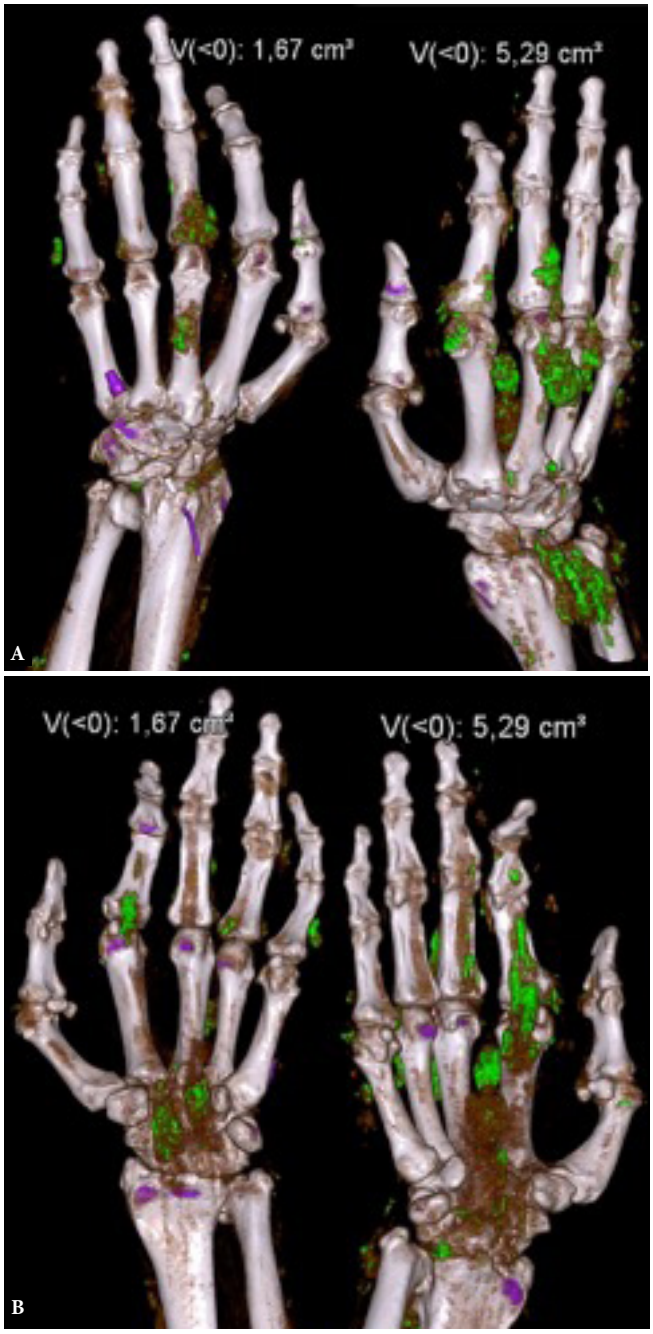

Fig. 7. *DECT of the hands in pronation (***A***) and in supination (***B***), year 2019. MSU crystal deposits are color-coded green*

In general, the already existing deposits enlarged. However, MSU crystal deposits occurred in new locations, including the tendon sheaths of the 2nd fingers, which caused their contraction.

US of the right hand showed synovial effusion and thickening without hyperemia of the synovial membrane in the MCP joints 1–5, in the IP joint of the thumb, in the tendon sheaths of the extensor tendons, and in the tendon sheath of the flexors in the 2nd and 3rd fingers. Small synovial calcifications were also identified in those locations (Fig. 10). A tophus was seen at the level of the 5th MCP joint of the right hand (Fig. 11).

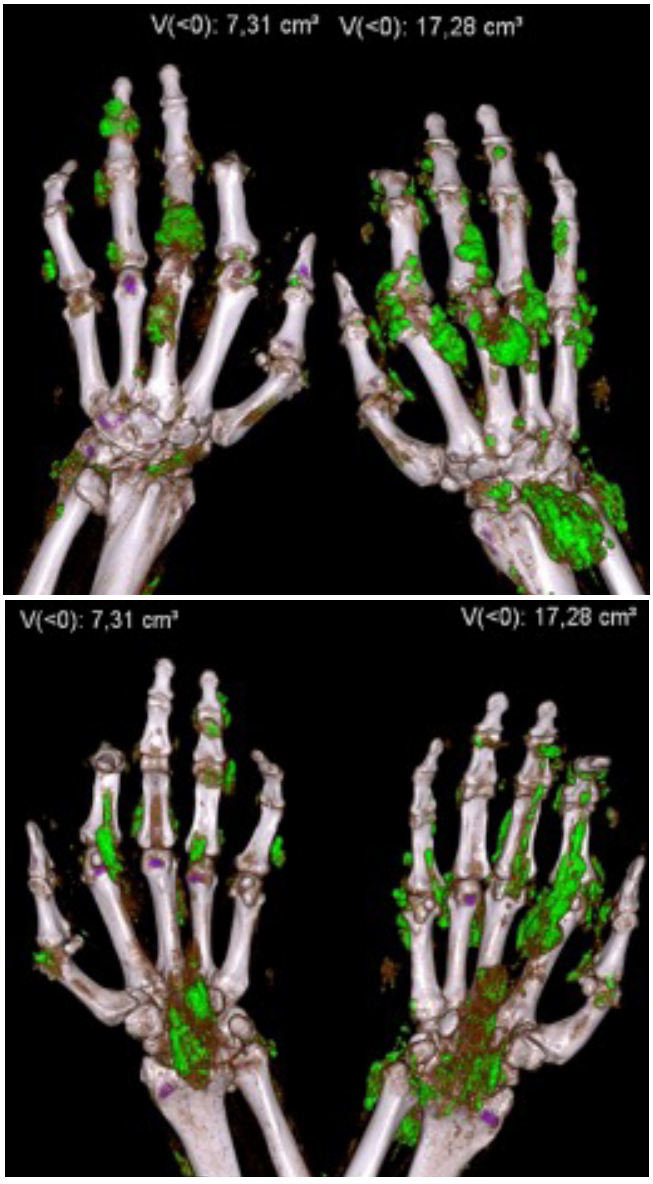

Fig. 9. *DECT of the hands in pronation (***A***) and in supination (***B***), year 2021. MSU crystal deposits are color-coded green*

Medical treatment was altered again, and allopurinol was replaced by febuxostat, still in combination with lesinurad. The patient was advised once more to modify his lifestyle.

In 2022, as a part of the patient's follow-up, DECT of the hands was performed again. It revealed a minimal increase in MSU deposit volume (left hand 1.65 cm^3, right hand 0.38 cm^3). This proved that the progression of the condition significantly slowed down.

Discussion

Gout has a number of imaging features that may be seen by ultrasound, radiographs, and DECT. Those vary according to the stage (early or chronic) of the disease (Tab. 1)[2]. In early gout radiographs, US, MRI and DECT findings are usually either non-specific or absent. Confirming the diagnosis at an early disease stage by visualizing needle-shaped negatively birefringent MSU crystals in synovial fluid on polarized light microscopy, which is a gold standard, may also be difficult. This is due to the fact that obtaining a sample for the test might be challenging during an early stage of the disease.

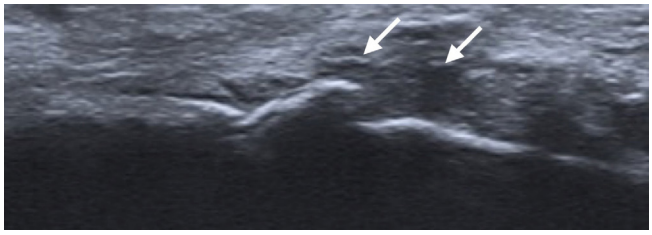

Fig. 10. *Ultrasound of the right 1st MCP joint, longitudinal view. Effusion and thickening of synovium with embedded small calcifications (a "starry sky" sign), arrows*

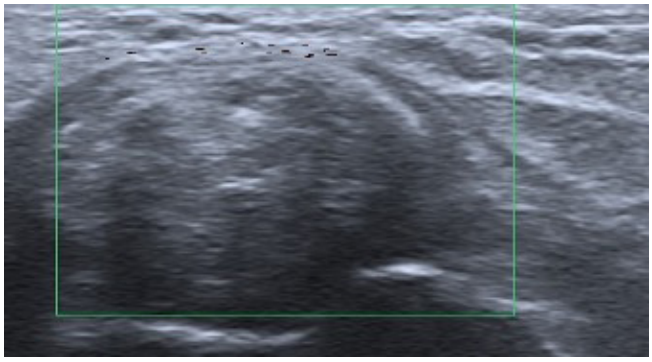

Fig. 11. *Hyperechoic tophus with tiny calcifications in the 5th MCP joint of the right hand, without increased vascularity, longitudinal view*

Early differential diagnosis may also be challenging. Other rheumatic inflammatory diseases, like peripheral spondyloarthropathies, rheumatoid arthritis or CPPD (calcium pyrophosphate dihydrate) also known as pseudogout, should be taken into account[2].

Specific radiographic findings of gout are often seen 6–15 years after the disease onset. These include characteristic erosions and tophi. In gout, erosions are juxta-articular with sclerotic margins and overhanging edges, joint spaces are spared, and periarticular bone density is intact. This finding is especially important when differentiating with rheumatoid arthritis, where erosions are most commonly located within joint spaces and occur earlier[9,10].

Ultrasound is a very valuable tool to visualize active and chronic inflammatory lesions of affected joints and periarticular soft tissues. They present as increased vascularity and swelling. These findings are non-specific and can occur in other inflammatory arthropathies[2].

This technique has been recognized by several societies/groups as an important instrument in the diagnostic process. OMERACT (Outcome Measures in Rheumatology) elaborated the consensus-based definitions of the four main elementary features of gout in ultrasound including erosions, tophi, aggregates and double contour sign[11].

The ACR (American College of Rheumatology) and EULAR (European Alliance of Associations for Rheumatology) classification criteria include US and DECT imaging features for the identification

Tab. 1. Radiological features of gout based on the imaging modality in early and chronic stages of the illness[2]

	Early stage	Chronic stage
Ultrasound	effusion synovial/tenosynovial hypertrophy bursitis starry sky sign (MSU deposits <1 mm) snowstorm sign/micro tophi (MSU aggregates >1 mm) double contour sign	tophi tendinopathy, tendons tears erosions
DECT	MSU crystal deposits detection and quantification	MSU crystal deposits detection and quantification
Radiography	asymmetric soft tissue swelling normal periarticular bone mineralization preservation of joint space rarely periostitis	erosions tophi pseudotumor pathological fracture normal periarticular bone mineralization preservation of joint space secondary osteoarthritis

of urate deposition in joints or bursae and for defining gout-related joint damage[5].

Tophi are the most characteristic sings of gout. On ultrasound, they may present as hyperechoic or hypoechoic nodules. They may be uniform or non-homogenous, may generate a posterior acoustic shadow, and may be surrounded by a small anechoic rim representing inflammation. They typically occur in regions of mechanical stress, but also around tendons (patellar, Achilles, quadriceps insertion), and in bursae[2].

The disadvantage of ultrasound is its inability to definitely differentiate MSU crystals typical for gout, from those found in CPPD or HA (hydroxyapatite) crystal deposition disease. However, according to the OMERACT analysis, there are certain typical locations for CPPD. The most affected joints, characterized by the highest prevalence of calcific deposits seen on ultrasound, were the menisci (90%), followed by the triangular fibrocartilage of the wrist (56%) and the knee hyaline cartilage (66%)[12]. Whereas for gout most common locations were feet, ankle and knee[2]. EFSUMB (European Federation of Societies for Ultrasound in Medicine and Biology) guidelines underline US capability to differentiate gout from CPPD deposition disease based on the distribution of crystals[13]. Deposits in CPPD tend to be hyperechoic. They can be seen in the middle layer of hyaline cartilage, within fibrocartilage and tendons, where they usually present in a linear form (multiple or single lines or a thick solid band)[14,15].

DECT is a fairly new computed tomography technique that allows the detection and quantification of MSU crystals. It relies on the fact that some materials, including MSU, have different attenuation at different energy levels. Data are typically acquired at 80 kV and 140 kV energy levels simultaneously. Later, the post-processing of data allows visualization of MSU crystals and their specific locations (joints, tendons, soft tissue)[16].

According to the meta-analysis performed by Ogdie *et al.*, DECT is an imaging modality with the highest specificity and sensitivity for gout (0.84 and 0.87). It was compared to the ultrasound double contour sign (0.76 and 0.83) and ultrasound tophus detection (0.80 and 0.65); see Tab. 2[17]. The advantages of this imaging technique in the early phase of gout include the detection of MSU crystal deposits as small as 2 mm. DECT has the ability to distinguish MSU deposits from others crystals, such as in CPPD. It reveals deposits in locations that are hard to reach during ultrasound examination. It is the only imaging method that can reliably and objectively assess the volume of MSU deposits, making it essential for disease follow-up. It may also visualize subclinical MSU deposits in patients without clinical evidence for acute gout. However, there are also disadvantages to this method, including false positive results due to artifacts. The most common artifacts occur in the nail bed and thickened skin. Other causes of false positive results could be advanced osteoarthritis, vascular calcifications, beam hardening, and image noise. False negative results may occur in early disease stages/ during the first gout attack due to microscopic tophi that are smaller than 2 mm in diameter and thus undetectable by DECT[18,19]. They can also be caused by urate lowering therapy or inadequate parameter settings[16].

Other imaging methods, such as magnetic resonance imaging (MRI) or computed tomography (CT), are rarely indicated in gout. MRI has proven its value when assessing the extent of joint, tendon, and bursal involvement, as well as, in diagnosis of gout complications such as tendon tears[20].

Summary

Gout imaging can be performed with several imaging methods, depending on the stage of the disease, the location of lesions, and the availability of equipment. Early changes in soft tissues are visible on both ultrasound and DECT. Advanced findings can be observed on DECT, ultrasound, and radiographs.

Ultrasound is widely available and performs well both for an acute and chronic gout. Ultrasound features of gout have been incorporated into the classification criteria of gout by ACR/EULAR, whereas OMERACT has prepared consensus-based definitions of the elementary features of gout in ultrasound, as mentioned earlier.

Tab. 2. Specificity and sensitivity of ultrasound and DECT in the diagnosis of gout based on Ogdie *et al.*[17]

	Specificity	Sensitivity
Ultrasound: Tophus	0.80	0.65
Ultrasound: Double contour sign	0.76	0.83
DECT: MSU crystal deposition	0.84	0.87

DECT enables both qualitative and quantitative assessment of the disease (crystals), and it is used for monitoring the course of disease and evaluation of the effectiveness of treatment, such as in the case presented above. Unfortunately, it is the least available technique, and false positive results are common due to artifacts, which should always be excluded from analysis by an experienced radiologist.

Conflict of interest

The authors do not report any financial or personal connections with other persons or organizations which might negatively affect the contents of this publication and/or claim authorship rights to this publication.

Author contributions

Original concept of study: MK, ANP, ISS. Writing of manuscript: MK, ANP, ML, ISS. Analysis and interpretation of data: MK, ANP, ML, ISS. Final approval of manuscript: MK, ANP, ISS, ML, ISS. Collection, recording and/or compilation of data: MK, ANP, ML. Critical review of manuscript: ISS.

References

1. Kuo CF, Grainge MJ, Zhang W, Doherty M: Global epidemiology of gout: Prevalence, incidence and risk factors. Nat Rev Rheumatol 2015; 11: 649–662. doi: 10.1038/nrrheum.2015.91.
2. Sudoł-Szopińska I, Afonso PD, Jacobson JA, Teh J: Imaging of gout: Findings and pitfalls. A pictorial review. Acta Reumatol Port 2020; 45: 20–25.
3. Dehlin M, Jacobsson L, Roddy E: Global epidemiology of gout: Prevalence, incidence, treatment patterns and risk factors. Nat Rev Rheumatol 2020; 16: 380–390. https://doi.org/10.1038/s41584-020-0441-1.
4. Zhang Y, Chen C, Choi H, Chaisson C, Hunter D, Niu J, Neogi T: Purine-rich foods intake and recurrent gout attacks. Ann Rheum Dis 2012; 71: 1448–1453. https://doi.org/10.1136/annrheumdis-2011-201215.
5. Neogi T, Jansen TL, Dalbeth N, Fransen J, Schumacher HR, Berendsen D *et al.*: 2015 Gout Classification Criteria: An American College of Rheumatology/European League against Rheumatism collaborative initiative. Arthritis Rheumatol 2015, 67, 2557–2568. doi: 10.1002/art.39254.
6. Spermon J, Van Dijke CF: Dual energy CT: Added value in gouty arthritis. JBR-BTR 2013 96: 34–37. doi: 10.5334/jbr-btr.179.
7. Grassi W, Okano T, Filippucci E: Use of ultrasound for diagnosis and monitoring of outcomes in crystal arthropathies. Curr Opin Rheumatol 2015; 27: 147–155. doi: 10.1097/BOR.0000000000000142.
8. Teh J, McQueen F, Eshed I, Plagou A, Klauser A: Advanced imaging in the diagnosis of gout and other crystal arthropathies. Semin Musculoskelet Radiol 2018, 22, 225–236. doi: 10.1055/s-0038-1639484.
9. Dalbeth N, Clark B, McQueen F, Doyle A, Taylor W: Validation of a radiographic damage index in chronic gout. Arthritis & Rheumatism 2007; 57: 1067–1073. doi: 10.1002/art.22891.
10. Martel W: The overhanging margin of bone: a roentgenologic manifestation of gout. Radiology 1968; 91: 755–756. doi: 10.1148/91.4.755. PMID: 5677514.
11. Gutierrez M, Schmidt WA, Thiele RG, Keen HI, Kaeley GS *et al.*: OMERACT Ultrasound Gout Task Force group. International Consensus for ultrasound lesions in gout: results of Delphi process and web-reliability exercise. Rheumatology (Oxford) 2015; 54: 1797–805. doi: 10.1093/rheumatology/kev112.
12. Adinolfi A, Sirotti S, Sakellariou G, Cipolletta E, Filippucci E, Porta F *et al.*: Which are the most frequently involved peripheral joints in calcium pyrophosphate crystal deposition at imaging? A systematic literature review and meta-analysis by the OMERACT ultrasound – CPPD subgroup. Front Med (Lausanne) 2023; 10: 1131362. doi: 10.3389/fmed.2023.1131362.
13. Naredo E, Rodriguez-Garcia SC, Terslev L, Martinoli C, Klauser A, Hartung W *et al.*: The EFSUMB Guidelines and Recommendations for Musculoskeletal Ultrasound – Part II: Joint Pathologies, Pediatric Applications, and Guided Procedures. EFSUMB-Leitlinien und -Empfehlungen für den muskuloskelettalen Ultraschall – Teil II: Gelenkpathologien, pädiatrische Anwendungen und geführte Verfahren. Ultraschall Med 2022; 43: 252–273. doi: 10.1055/a-1640-9183
14. Filippou G, Adinolfi A, Iagnocco A, Filippucci E, Cimmino MA, Bertoldi I *et al.*: Ultrasound in the diagnosis of calcium pyrophosphate dihydrate deposition disease. A systematic literature review and a meta-analysis. Osteoarthritis Cartilage 2016; 24: 973–981. doi: 10.1016/j.joca.2016.01.136.
15. Omoumi P, Zufferey P, Malghem J, So A: Imaging in gout and other crystal-related arthropathies. Rheum Dis Clin North Am 2016; 42: 621–644. doi: 10.1016/j.rdc.2016.07.005.
16. Chou H, Chin TY, Peh WC: Dual-energy CT in gout – A review of current concepts and applications J Med Radiat Sci 2017; 64: 41–51. doi: 10.1002/jmrs.223.
17. Ogdie A, Taylor WJ, Weatherall M, Fransen J, Jansen TL, Neogi T *et al.*: Imaging modalities for the classification of gout: Systematic literature review and meta-analysis. Ann Rheum Dis 2015; 74: 1868–1874. doi: 10.1136/annrheumdis-2014-205431.
18. Mallinson PI, Coupal T, Reisinger C, Chou H, Munk PL, Nicolaou S, Ouellette H: Artifacts in dual-energy CT gout protocol: A review of 50 suspected cases with an artifact identification guide. AJR Am J Roentgenol 2014; 203: W103–W109. doi: 10.2214/AJR.13.11396.
19. Jia E, Zhu J, Huang W, Chen X, Li J: Dual-energy computed tomography has limited diagnostic sensitivity for short-term gout. Clin Rheumatol 2018; 37: 773–777. doi: 10.1007/s10067-017-3753-z.
20. Sahu AK, Kataria S, Gandikota G. Added value of high-resolution ultrasound and MRI in the evaluation of rheumatologic diseases. J Ultrason 2023; 23: e285-e298. doi: 10.15557/jou.2023.0035.